EXPERIMENTAL STUDY OF AN ORC WITH UNCERTAINTY ANALYSIS AND INTER-MODEL COMPARISON FOR THERMODYNAMIC PROPERTIES OF R1233ZD-E

Sebastian Eyerer[1,*], Wei Liu[1], Matthäus Irl[1], Stefan Ausfelder[1], Eva-Maria Dichtl[1], Christoph Wieland[1], Hartmut Spliethoff[1,2]

[1] Institute for Energy Systems, Faculty of Mechanical Engineering, Technische Universität München, Boltzmannstr. 15, 85748 Garching, Germany.

[2] The Bavarian Center for Applied Energy Research (ZAE Bayern), Division 1: Technology for Energy Systems and Renewable Energy, Walther-Meissner-Str. 6, 85748 Garching, Germany

* Corresponding Author, Tel. +49 89 289 16264, Fax. +49 89 289 16271, Email address: sebastian.eyerer@tum.de

Link to pdf: http://mediatum.ub.tum.de/node?id=1304849

ABSTRACT

This study analyzes an experimental investigation of an Organic Rankine Cycle (ORC) with R1233zd-E as working fluid in terms of measuring uncertainty. A methodology for an uncertainty analyses containing systematic errors and the propagation of random errors has been presented and exemplarily applied for the measuring uncertainty of the gross thermal efficiency. There, the uncertainty calculated from the manufacturers' data sheet uncertainties and the measured uncertainties calculated with the empirical standard deviation have been compared resulting in the observation, that the empirical standard deviation is less for all experiments. Furthermore, the influence of using different Equation Of States (EOS) for the calculation of thermodynamic properties has been analyzed. It can be concluded, that the deviation between the Helmholtz-Energy EOS and the Peng-Robinson EOS is in the same order of magnitude as the measurement uncertainty.

1. INTRODUCTION

In recent years, interests on the utilization of low temperature heat have grown rapidly due to the aim of increasing energy efficiency and the proportion of renewable energy sources. Therefore, the ORC is one of the most promising technologies. Instead of water, as it is used in the conventional Rankine cycle, the ORC uses an organic working fluid. Due to the environmental impact of many state-of-the-art fluids, hydrofluoroolefins as the so called fourth generation of working fluids have been developed. One representative of this group is R1233zd-E which is said to be a drop-in replacement for R245fa (*Eyerer et al*, 2016), a currently wide spread refrigerant in ORC with a significant global warming potential (GWP).

For the evaluation of measured quantities from an experimental study, fluid properties are commonly obtained from a well-established fluid database such as REFPROP which employs multi-parameter EOS for calculation. Contrary to that, the thermodynamic properties can also be determined with another EOS such as the cubic Peng-Robinson (PR) EOS. Both approaches have a specific uncertainty in defining the required properties and thus affects the finally calculated quantities.

In the present study an experimental investigation of an ORC with R1233zd-E as working fluid is conducted. Thereby, the purpose of this work is twofold: First, focus is put on the uncertainty analyses of the measured parameter and the subsequent error propagation. Second, the differences associated with the use of two different EOS for the calculation of thermodynamic properties are analyzed and discussed.

2. EXPERIMENTAL FACILITY AND METHODOLOGY

The ORC test rig has a standard cycle design and consists of two major loops, a heating loop where pressurized water circulates and an ORC loop where working fluid flows. The schematic view of the test rig as well as the applied measurement devices and major control options are depicted in *figure 1*. For data acquisition and test rig control the reconfigurable control system CompactRIO by National Instruments together with the system design software LabVIEW is applied.

The heat source of the ORC is a 45kW electrical resistance heater whose power is controlled by pulse width modulation. A semi-hermetic automobile scroll compressor from Sanden International, Inc. has been modified to work as an expander. A positive displacement reciprocating diaphragm pump is used as a feed pump for the cycle. And an air-cooled condenser is applied as the heat sink of the system.

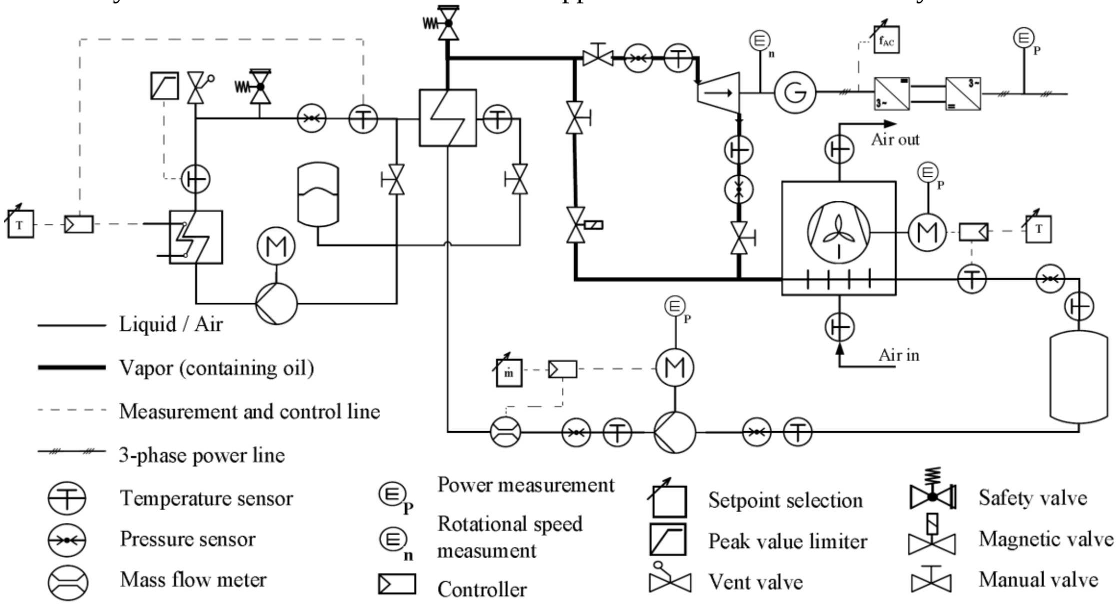

Figure 1: Schematic view of the ORC test rig

For experimental investigation the mass-flow rate of the working fluid is varied while all other operational parameters are kept constant. Therefore, the heat source temperature is set to 120 °C with a constant water mass-flow. The rotational speed of the expander is set to 3000 rpm and the condensation temperature is controlled to a value of 25 °C. With this constant condition, the working fluid mass-flow rate is increased from 15 g/s up to 45 g/s in 5 g/s steps. Due to a fixed condensation temperature, the increasing mass flow rate leads to a higher live steam pressure and thus a higher pressure ratio (*Eyerer et al*, 2016). For all seven operating points, stationary conditions are maintained for at least 5 min. For evaluation of the measuring uncertainty an interval of 20 s has been used containing $n = 20$ values.

For the evaluation of the measured parameter, the uncertainty of the respective measurement device is considered in two ways. First, the device uncertainties are extracted from the manufacturers' data sheets (cf. table 1) and second compared to the random errors obtained when measuring at stationary conditions accounting for different confident bounds. Using these uncertainties of each parameter, the error propagation for calculated values such as thermodynamic properties and system parameters is obtained by applying the Gaussian law of error propagation.

Table 1: Measuring range and accuracy of relevant sensors from the manufacturers' data sheets

Measured Parameter	measurement principle	Measuring Range	Measurement accuracy
Live steam pressure	Strain gauge	0…25 bar_{rel}	0.5% MV + 1.3% EV
Exhaust steam pressure	Strain gauge	0…16 bar_{rel}	0.5% MV + 1.3% EV
Feed pressure	Strain gauge	0…16 bar_{rel}	0.5% MV + 1.3% EV
Live steam temperature	PT100	-50…200 °C	0.05% MV + 0.3 °C
Exhaust steam temp.	Thermocouple Typ K	-200…1372 °C	1.5 °C
Feed temperature	Thermocouple Typ K	-200…1372 °C	1.5 °C
Mass-flow rate	Coriolis sensor	0.5…25 kg/min	0.04 kg/min
Electrical output power	Power meter	0…3000 W	1% MV

In the present study, the gross thermal efficiency $\eta_{th,gross}$ is analyzed exemplarily as a major characteristic system parameter.

$$\eta_{th,gross} = \frac{P_{el}}{\dot{m}_{WF}(h_{LS} - h_F)} = \frac{P_{el}}{\dot{Q}_{sup}} \qquad [1]$$

This parameter requires a multi-step calculation from the measured parameter temperature, pressure and mass-flow rate as well as the application of an EOS for enthalpy and entropy calculation and is thus suitable for the purpose of this study.

3. CALCULATION OF THERMODYNAMIC PROPERTIES

The calculation of thermodynamic properties is based on two types of EOS. First, the Helmholtz-Energy (HE-) EOS is selected as the benchmark due to its high accuracy of calculation (*Mondéjar et al*, 2015). Second, a cubic EOS, namely the Peng-Robinson (PR-) EOS is considered due to its simplicity and sufficient accuracy for engineering purposes (*Peng and Robinson*, 1976). For the HE-EOS, the ideal-gas isobaric heat capacity is obtained using the Plank-Einstein term, based on theoretical estimates and experimental data (*Mondéjar et al*, 2015), while for the PR-EOS it is calculated with a polynomial term, based on the density functional theory (*Hulse et al*, 2012). For numeric calculations, the HE-EOS is implemented in REFPROP (*Lemmon et al*, 2013), while the PR-EOS in OFluid (*Liu et al.*, 2014).

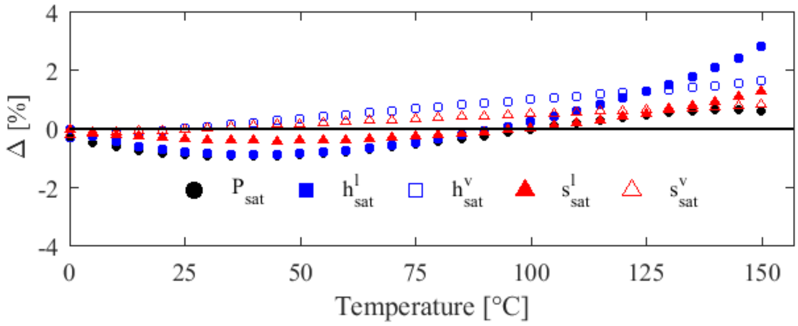

Figure 2: Percentage deviations in saturation properties obtained with PR-EOS as a function of temperature for R1233zd-E

The choice of EOS has direct impacts on fluid properties, which could influence cycle evaluations (*Heberle et al.*, 2015). Figure 2 shows typical percentage deviations in saturation properties calculated with the PR-EOS as a function of temperature for R1233zd-E. Thereby, the deviation is defined as $\Delta = \frac{y_{HE} - y_{PR}}{y_{HE}}$. It can be observed that deviations are large (up to 3.04%) at high temperatures especially for the calorific properties. The deviation of 3.21% between the considered heat capacity models can be regarded as the main reason for the high deviations in figure 2 (*Mondéjar et al,* 2015). Such deviations could lead to considerable uncertainties with regard to the calculated cycle characteristics such as thermal efficiencies. In a next step, the deviations of the fluid properties obtained by the model comparison are compared with the measurement uncertainties resulting in a better understanding of accuracy of measurement.

4. UNCERTAINTY ANALYSIS

Measurement errors can be divided into two groups, the systematic errors and the random errors. While the systematic errors cause an offset to the true value, the random errors scatter around a mean value. Due to the reproducibility of the offset, systematic errors can be corrected or reduced in influence by calibrating the measuring system. In this case, the used sensors are dismantled from the test rig in order to expose them to a defined state. The temperature sensors are therefore put in a stirred water bath which is heated up from 20 °C to 90 °C in steps of 10 K. The measured values are compared with the reading of a high precision, manufacturer calibrated, resistance thermometer (accuracy of 0,03 °C). Occurring deviations are then corrected by a linear least square fit. In the case of pressure sensors, a similar procedure is applied using a high precision manometer (accuracy of 0,1 bar) as reference and a pneumatic hand pump as pressure source. There, the pressure is increased in steps of 1 bar within the full measuring range of each sensor. For which, the temperature and the pressure sensors, it is important, that the same data acquisition system is used for calibration and real measurement. Then, possible systematic errors of the wiring and the data acquisition system are also being corrected.

In contrast to the systematic errors, random errors are not reproducible and thus, cannot be corrected. However, this kind of error can be characterized by statistical methods which are valid for normally distributed events. In the case of measurements, this requirement is often satisfied but should be verified before application. In general, the statistical population has to be delimited from a series of measurements. While the population describes the entirety of normally distributed values, a series of measurements is only a sample of this population. The series of measurements can statistically be described by the arithmetic average $\bar{x} = \frac{1}{n}\sum_{i=1}^{n} x_i$ and the empirical standard deviation:

$$\sigma_x = \sqrt{\frac{1}{n-1}\sum_{i=1}^{n}(x_i - \bar{x})^2}\,. \qquad [2]$$

However, the calculated arithmetic average $\bar{x}$ as well as the empirical standard deviation σ_x are only estimators for the true value x_0 and standard deviation of the entire population σ_0. Describing a series of measurements by its arithmetic average $\bar{x}$ and its empirical standard deviation σ_x means, that the next measured value lies with a probability of 68,3 % within the range of $\bar{x} \pm \sigma_x$. Other typical confidence intervals are 95,5 % and 99,7 % corresponding with a range of $\pm 2\sigma_x$ and $\pm 3\sigma_x$. However, the quantity of interest is a range, in which the true value x_0 can be found. This is described by the standard deviation of the mean value $\sigma_{\bar{x}} = \frac{\sigma_x}{\sqrt{n}} t$. Here, the factor t considers the uncertainty of the empirical standard deviation of the measurement series. This quantity is student-t-distributed and varies depending on the number of measurements within a sample n and the considered confidence level. Therefore, it is important to know the selected confidence interval.

In most cases, the measured values are used to calculate the desired quantities, e.g. the thermal efficiency. In order to quantify the uncertainty of this derived quantity, the Gaussian law of error propagation can be applied. When the quantity of interest y can be obtained by independent measured quantities x_j with a physical correlation in the form of $y = f(x_1, x_2, \ldots, x_k)$ the standard deviation of the derived quantity σ_y is described by:

$$\sigma_y = \sqrt{\sum_{j=1}^{k}\left(\frac{\partial f}{\partial x_j}\sigma_{\bar{x}_j}\right)^2}\,. \qquad [3]$$

When the physical correlation f is not described in a direct analytical manner, which is the case for both used EOS, the derivation $\frac{\partial f}{\partial x_j}$ is obtained as a central difference quotient. In the case of calculating the measurement uncertainties by means of the device uncertainties extracted from the manufacturers' data sheets, equation 3 is applied by using the device uncertainties as standard deviation of the mean value $\sigma_{\bar{x}_j}$.

5. FINDINGS AND CONCLUSION

The experiments described in section 2 has been evaluated in terms of gross thermal efficiency $\eta_{th,gross}$ The efficiencies depicted in figure 3 are calculated by using the Helmholtz-Energy EOS.

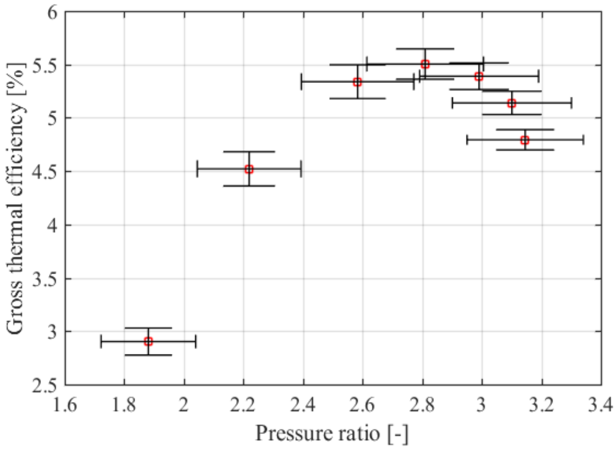

Figure 3: Gross thermal efficiency as a function of the expanders pressure ratio

The red squares indicate the experimental mean values $\bar{\eta}_{th,gross}$ and the error bars indicate the measuring uncertainty calculated by using the manufacturers' data sheet uncertainties. The maximum gross thermal efficiency is 5.5 % with an absolute uncertainty of $\sigma_{\overline{\eta}_{th,gross}} = 0.1$ % and a relative uncertainty of $\frac{\sigma_{\overline{\eta}_{th,gross}}}{\overline{\eta}_{th,gross}} = 2.6$ %. Comparing the discussed sources of uncertainties for defining the gross thermal efficiency, figure 4 depicts both the relative and absolute uncertainty calculated from the manufacturers' data sheet uncertainties, the measured uncertainties calculated with the empirical standard deviation of the mean value $\sigma_{\overline{\eta}_{th,gross}}$ as well as the deviation Δ obtained when calculating the thermodynamic properties with different EOS. The confidence interval is set to 99.7 %.

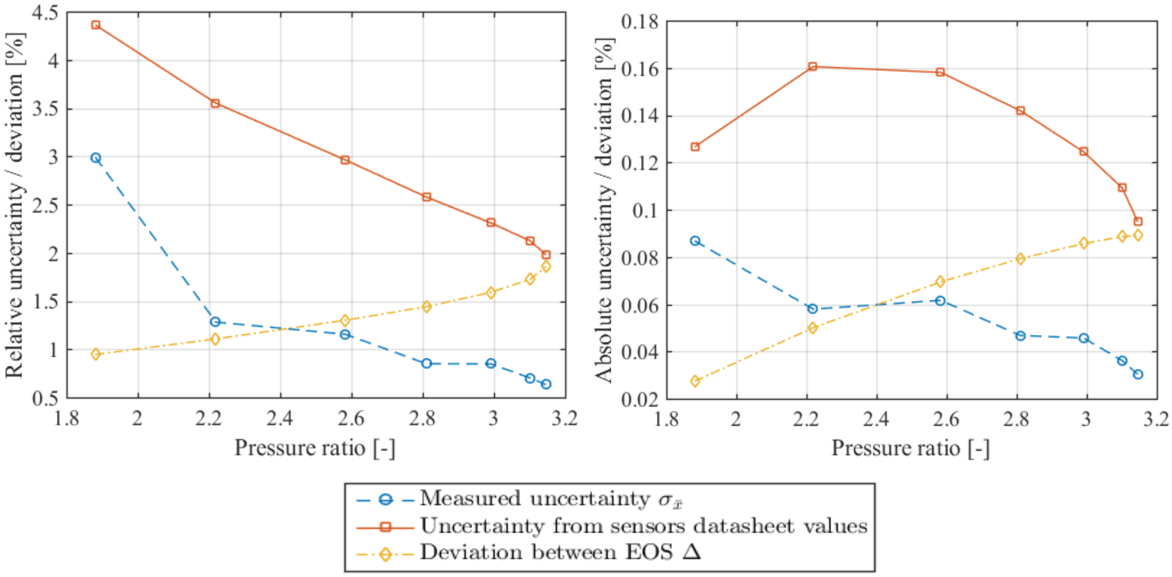

Figure 4: Comparison of the measurement uncertainty and the deviation between both EOS

Comparing the uncertainty calculated from the manufacturers' data sheet uncertainties with the measured uncertainty, it can be seen in figure 4, that the empirical uncertainty (blue dashed line) is less for both, the relative and the absolute values. An interesting fact is, that the relative data sheet uncertainty decreases with higher pressure ratios. This is due to an increasing mean values of the live steam state. The deviation between both EOS however, is increasing with pressure ratio. The relevant quantity for this deviation is the determination of the enthalpy which is less accurate for high temperatures and pressures (cf. section 2). Furthermore, it can be concluded from figure 4, that the deviation between the HE-EOS and the PR-EOS is in the same order of magnitude as the measurement uncertainty.

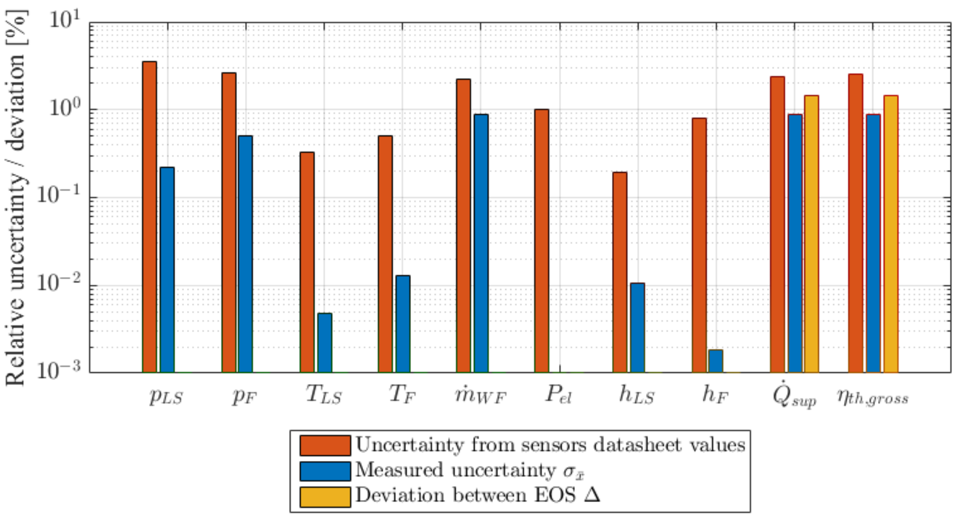

Figure 5: Error propagation for the calculation of the gross thermal efficiency

In order to further analyze the influence of the error propagation from the measured to the derived quantities, figure 5 shows the relative uncertainty of each quality during the calculation of the gross thermal efficiency. Here, the deviation between the EOS is only considered in the last two steps. The direct comparison of the enthalpy calculation is not possible because the calorific properties are normalized. Thus, only the enthalpy difference is a meaningful quantity. From this analyses, it can be concluded, that the pressure measurements are most influencing the final result of the gross thermal efficiency because these values have a high measuring error which is propagated in the enthalpy calculation.

ACKNOWLEDGMENT

Funding from the Bavarian State Ministry of Education, Science and the Arts in the frame of the project Geothermie-Allianz Bayern is gratefully acknowledged.

NOMENCALTURE

Latin symbols

EV	end value
h	specific enthalpy [kJ/kg]
k	number of influencing variables of a derived quantity
$\dot{m}$	mass-flow rate [g/s]
MV	measured value
n	number of measurements in one series
P	power [W]
$\dot{Q}$	Heat flow [kW]
x	Measured value
x_0	true value
$\bar{x}$	arithmetic average of measurements
y	derived quantity

Greek symbols

σ_0	standard deviation of the entire population
σ_x	empirical standard deviation
$\sigma_{\bar{x}}$	empirical standard deviation of the mean value

Further subscripts

el	electrical
ES	exhaust steam
F	feed
$gross$	gross
i	index of measurements within a series
is	isentropic
j	index of influencing variables of a derived quantity
LS	live steam
sup	supply
th	thermal
WF	working fluid

REFERENCES

Coleman, H.W.; Experimentation, Validation, and Uncertainty Analysis for Engineers, John Wiley & Sons, 2009.

Eyerer, S.; Wieland, C.; Vandersickel, A.; Spliethoff, H.; Experimental study of an ORC (Organic Rankine Cycle) and Analysis of R1233zd-E as a Drop-In Replacement for R245fa for low Temperature Heat Utilization. *Energy*, Vol. 103, pp. 660-671, 2016.

Heberle, F.; Jahrfeld, T.; Brüggemann, D.; Thermodynamic Analysis of Double-Stage Organic Rankine Cycles for Low-Enthalpy Sources Based on a Case Study for 5.5 MWe Power Plant Kirchstockach (Germany), *Proceedings World Geothermal Congress*, 2015.

Hulse, R. J.; Basu, R. S.; Singh, R. R.; Thomas, R. H.; Physical properties of HCFO-1233zd (E). *Journal of Chemical & Engineering Data*, Vol. 57 (12), pp. 3581-3586, 2012.

Lemmon, E.W.; Huber, M.L.; McLinden, M.O.; NIST Reference Fluid Thermodynamic and Transport Properties-REFPROP. NIST Standard Reference Database 23-Version 9.1, 2013.

Liu, W.; Meinel, D.; Wieland, C.; Spliethoff, H.; Investigation of Hydrofluoroolefins as Potential Working Fluids in Organic Rankine Cycle for Geothermal Power Generation. *Energy*, Vol. 67, 2014.

Mondéjar, M. E.; McLinden, M. O.; Lemmon, E. W.; Thermodynamic Properties of trans-1-Chloro-3, 3, 3-trifluoropropene (R1233zd (E)): Vapor Pressure, (p, ρ, T) Behavior, and Speed of Sound Measurements, and Equation of State. *Journal of Chemical & Engineering Data*, Vol. 60 (8), pp. 2477-2489, 2015.

Peng, D. Y.; Robinson, D. B.; A new Two-Constant Equation Of State. *Industrial & Engineering Chemistry Fundamentals*, Vol. 15 (1), pp. 59-64, 1976.